DFT study on the regeneration mechanism of ZnO surface during the desulfurization of H_2S

Lixia Ling [a,b], Peide Han [b], Baojun Wang [c,*], Riguang Zhang [c]

[a] Research Institute of Special Chemicals, Taiyuan University of Technology, Taiyuan 030024, Shanxi, PR China
[b] College of Materials Science and Engineering, Taiyuan University of Technology, Taiyuan 030024, Shanxi, PR China
[c] Key Laboratory of Coal Science and Technology (Taiyuan University of Technology), Ministry of Education and Shanxi Province, Taiyuan 030024, Shanxi, China

ARTICLE INFO

ABSTRACT

The regeneration mechanisms of the sulfurized and oxygen-deficient $ZnO(10\bar{1}0)$ surfaces in an oxygen atmosphere have been systematically studied by using the density functional theory (DFT) method. An activation energy of 36.79 kJ·mol^{-1} is needed for the regeneration of the sulfurized $ZnO(10\bar{1}0)$ surface at the GGA–PW91 functional level. The formed SO_2 lies on the $ZnO(10\bar{1}0)$ surface horizontally, S in SO_2 bonds to a surface oxygen atom to form an analogical SO_3 structure. Two regeneration mechanisms are studied for the oxygen-deficient $ZnO(10\bar{1}0)$ surface. One is that O_2 dissociatively adsorbs on the oxygen-deficient $ZnO(10\bar{1}0)$ surface leading to the regeneration of the surface. The other is that O_2 molecularly adsorbs on the oxygen-deficient $ZnO(10\bar{1}0)$ surface, then a little activation energy of 29.43 kJ·mol^{-1} is needed to make the surface regenerate. It can be concluded that the sulfurized and oxygen-deficient $ZnO(10\bar{1}0)$ surfaces are easy to be regenerated in an atmosphere containing O_2.

© 2012 Elsevier B.V. All rights reserved.

1. Introduction

Zinc oxide (ZnO) is the most widely used desulfurizer to remove sulfur species such as H_2S from gas streams due to its negative effects on environment and chemical processing [1,2]. Sulfidation is the first process during the desulfurization. In this process, S can be deposited on the surface leading to the loss of sulfidation activity of ZnO, thereby influencing the desulfurization capacity. On the other hand, the formation of H_2O results in an oxygen vacancy on the surface, which has the influence on the lifetime of ZnO if the oxygen vacancy had not been filled. A good desulfurizer not only has the combination of a high affinity towards the reaction with H_2S, but also the formation of a sulfide which can be converted back to the oxide through oxidation [3]. It is obvious that the regenerability is an important property of desulfurizer [4], which influences the desulfurization capacity and lifetime of desulfurizer.

The desulfurized material of ZnO supported on TiO_2 was prepared by Elseviers et al. [3]. The regeneration thermodynamic equilibrium has been simulated using Aspen Plus, and it can be concluded that the material can be regenerated completely at 600 °C. Bulk Zn–Ti–O binary oxides were synthesized by adding TiO_2 into ZnO to stabilize ZnO, and cyclic sulfidation-regeneration experiments were performed in a packed-bed microreactor. It showed that the intrinsic sulfidation kinetics of zinc titanates was similar to zinc oxide at 650 °C, and the sulfided

zinc titanate sorbents were fully regenerationable [5]. The above experiments show that zinc sulfide can be regenerated. A free oxygen-containing gas is needed to be introduced to the reactor for the purpose of oxidizing the zinc sulfide [6]. The regeneration performance of ZnO has been investigated by Focht et al. [7], and the result showed that an oxygen atmosphere gives the following regeneration reaction: $ZnS + (3/2)O_2 \rightarrow ZnO + SO_2$. Other investigators agreed with this reaction process [8,9]. A fundamental understanding of the regeneration mechanism is important for two reasons. First, experimental information is however not always sufficient and accompanying theoretical calculations can be helpful to clarify some questions. And, second, the regeneration of the oxygen-deficient surface has not been studied.

About the regeneration process in an atmosphere containing O_2, the adsorption and dissociation of O_2 on the perfect and deficient surfaces are important. With recent development, density functional theory (DFT) method has already been extensively used to study the adsorption of O_2 on the different perfect surfaces MgO(001) [10,11], SnO_2(110) [12], Cu_2O(100) [13], Cu_2O(111) [14] and deficient Cu_2O(111) surface [14]. To the best of our knowledge, few theoretical studies about the adsorption of O_2 on the oxygen-deficient $ZnO(10\bar{1}0)$ surfaces have been systematically reported, which will be helpful to deeply probe into the regeneration process at a microscopic level. Only Yan et al. [15] investigated the interaction of O_2 on the periodic oxygen-deficient $ZnO(10\bar{1}0)$ slab with the bottom side passivated by hydrogen atoms, however, no hydrogen atoms are passivated on the $ZnO(10\bar{1}0)$ slab in experiment [16,17] and in other theoretical studies [18,19]. And no theoretical study about the adsorption of O_2 on the sulfide $ZnO(10\bar{1}0)$ surface has been reported.

* Corresponding author at: No. 79 Yingze West Street, Taiyuan 030024, China. Tel.: +86 351 6018239; fax: +86 351 6041237.
E-mail address: wangbaojun@tyut.edu.cn (B. Wang).

Following the sulfidation process during the desulfurization of H_2S reported in the former study [20], the regeneration mechanisms in the presence of O_2, including the sulfurized $ZnO(10\bar{1}0)$ surface and the oxygen-deficient $ZnO(10\bar{1}0)$ surface are microscopically studied by using the periodic density functional theory (DFT) method. Meanwhile, the adsorptions of O_2 molecule on the perfect and oxygen-deficient $ZnO(10\bar{1}0)$ surfaces, SO_2 and O atom on the perfect $ZnO(10\bar{1}0)$ surface are investigated to obtain the stable intermediates. The activation energies for the regeneration processes are also calculated, which may be of interest to researchers attempting to explore the better desulfurizers.

2. Computational modes and methods

2.1. Surface models

The sulfurized and oxygen-deficient $ZnO(10\bar{1}0)$ surfaces were constructed according to the perfect $ZnO(10\bar{1}0)$ surface. The perfect $ZnO(10\bar{1}0)$ surface was modeled with 6 atomic layer slab and a $p(2\times2)$ supercell; a vacuum region of 1 nm thickness was used to separate the surface from its periodic image in the direction along the surface normal (z direction). The optimized $ZnO(10\bar{1}0)$ surface is shown in Fig. 1(a) and (b). Meanwhile, considering the effect of layers on the surface and the electronic coupling between the adjacent slabs, an 8 layer slab model and a more large size model $p(3\times2)$ supercell were used to calculate the adsorption energy of H_2S on the $ZnO(10\bar{1}0)$ surface; the energy differences were only 1.29 kJ·mol^{-1} and 3.12 kJ·mol^{-1} corresponding to the 6 layer slab with $p(2\times2)$ supercell, respectively.

The sulfurized $ZnO(10\bar{1}0)$ surface was constructed by a S atom bridging a $Zn-O$ bond on the perfect $ZnO(10\bar{1}0)$ surface. It is the most stable structure, as shown in Fig. 1(c) and (d). Other two structures of S atom bridging Zn and O in parasites of a hexagonal channel and S atom bonding to two adjacent Zn atoms on the perfect $ZnO(10\bar{1}0)$ surface were also investigated; the adsorption energies of which

were lower than that of the most stable structure by 12.96 and 88.66 kJ·mol^{-1}, respectively.

The removal of the oxygen at the top atomic layer from the perfect surface results in what was called the oxygen-deficient $ZnO(10\bar{1}0)$ surface [21], as shown in Fig. 1(e) and (f). Zn3, Zn5 and Zn6 atoms used to bond with O3, are now Zn3 and Zn5, Zn3 and Zn6 bond with each other, respectively. The Zn3 atom is on the surface, but the Zn5 and Zn6 atoms are below the surface.

In all calculations the bottom two layers of the slab were kept fixed at their bulk-like position, while the remaining atoms in the top four layers, and the adsorbed molecules/or atoms were allowed to move.

2.2. Calculation methods

The calculations were performed using the density functional theory (DFT) method [22,23], where the generalized gradient approximation (GGA) corrected the exchange-correlation functional proposed by Perdew and Wang [24,25] was chosen together with the doubled numerical basis set plus polarization basis sets (DNP) [26]. The inner electrons of Zn atom were kept frozen and replaced by an effective core potential (ECP) [27], and other atoms were treated with an all-electron basis set. Brillouin-zone integrations were performed using $4\times2\times1$ Monkhorst-Pack grid. A Fermi smearing of 0.005 hartree and a real-space cutoff of 4.4 Å were used to improve the computational performance. Spin unrestricted was performed. The tolerances of energy, force, and displacement convergence were 2×10^{-5} hartree, 4×10^{-3} hartree/Å, and 5×10^{-3} Å, respectively. All calculations were carried out with the Dmol^3 program package [28,29] on HP Proliant DL 380 G5 server system.

The adsorption energies, E_{ads}, are calculated as follows:

$$E_{ads} = E_{tot}(ads) + E_{tot}(slab) - E_{tot}(ads/slab)$$

where $E_{tot}(ads)$ is the total energy of the free adsorbate in the gas phase, $E_{tot}(slab)$ is the total energy of the bare slab, and $E_{tot}(ads/$

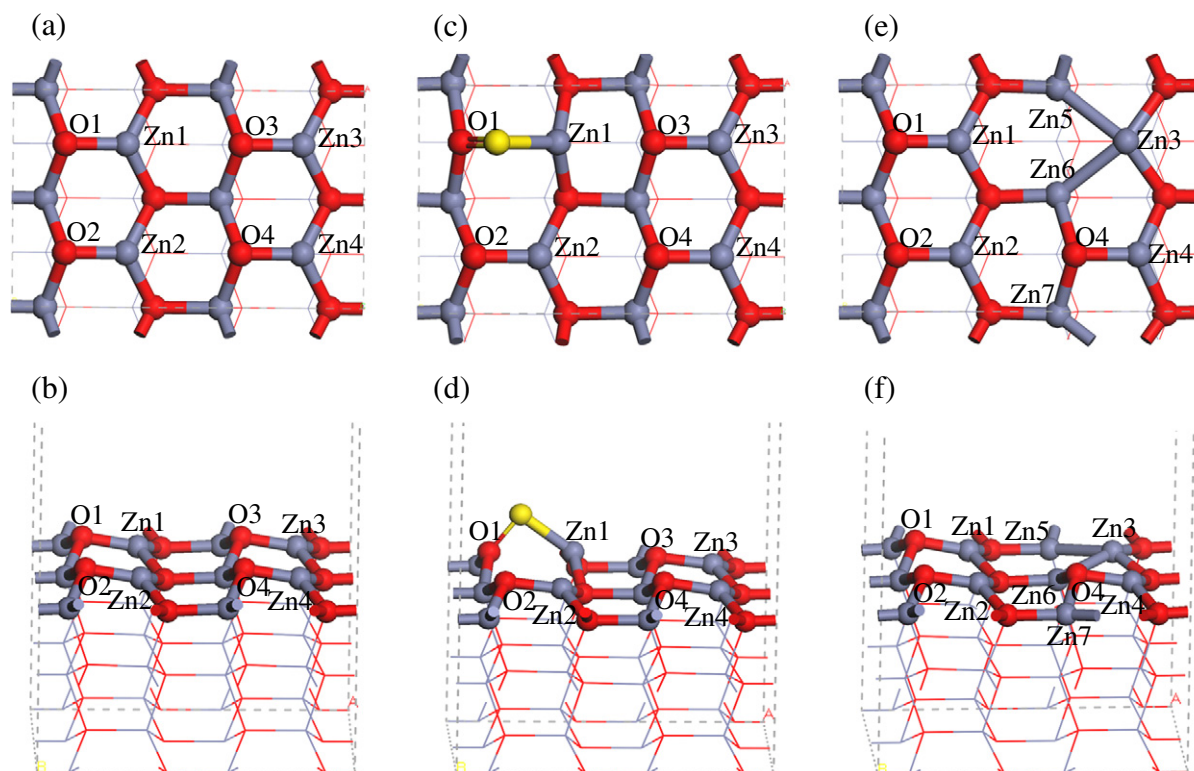**Fig. 1.** The slab models of $ZnO(10\bar{1}0)$ surface.

slab) is the total energy for the slab with adsorbate in its equilibrium geometry.

Transition state (TS) search was performed at the same theoretical level with the complete linear synchronous transit/quadratic synchronous transit (LST/QST) method [30]. In addition, TS confirmation was performed on every transition state structure to confirm that they lead to the desired reactants and products using the nudged elastic band (NEB) method.

The activation energy (E_a) is defined as follows:

$$E_a = E_{tot}(TS) - E_{tot}(R)$$

where $E_{tot}(R)$ is the total energy of reactant in every elementary reaction, and $E_{tot}(TS)$ is the total energy of transition state in every elementary reaction.

3. Results and discussion

3.1. Calculations of O_2 molecule and bulk ZnO

The bond length of molecular O_2 calculated from our approach is r(O–O) = 0.1225 nm, which is in good agreement with the experimental value of 0.1207 nm [31], as well as the other similar GGA results [32]. Then, the test is to predict the lattice constant of bulk ZnO. The calculated values for the lattice constants are a = b = 0.3306 nm and c = 0.5326 nm in comparison with the experimental value of a = b = 0.3249 nm and c = 0.5205 nm [33], the largest deviations of calculation value from the experimental value are only 1.75 and 2.32%, respectively. The calculated values are also in good agreement with the other similar GGA results [34]. These results obtained in above tests make us confident in pursuing the regeneration mechanisms of the sulfurized and oxygen-deficient ZnO(10$\bar{1}$0) surfaces in an atmosphere containing O_2.

3.2. Adsorption of O_2 molecule on the perfect ZnO(10$\bar{1}$0) surface

In order to study the regeneration mechanism of the sulfurized ZnO(10$\bar{1}$0) surface, what to be investigated first is the adsorption of O_2 on a stoichiometric ZnO(10$\bar{1}$0) surface. The optimized perfect ZnO(10$\bar{1}$0) surface is that the surface consists of slightly tilted ZnO "dimmers" with 9.899° as indicated in Fig. 1(a) and (b), which is in agreement with the other calculation results [35] and experimental results by Duke et al. [36]. The Zn and O atoms on the surface are threefold coordinated.

Three adsorption configurations of O_2 molecule on the perfect ZnO(10$\bar{1}$0) surface are obtained, which are named as O_2(a), O_2(b) and O_2(c), as shown in Fig. 2. The adsorption energies are listed in Table 1. O_2(a) is the O_2 molecule bonding to two neighboring Zn atoms on the surface, forming a bridging O_2 molecule. The formed Oa–Zn1 and Ob–Zn2 bonds are 0.2212 and 0.2214 nm, respectively. The O–O bond length of the O_2 molecule is 0.1289 nm, which is stretched slightly by 0.0064 nm corresponding to 0.1225 nm of O_2 molecule in gas phase. Yan et al. [15] have also investigated the adsorption of O_2 on the perfect ZnO(10$\bar{1}$0) surface, the calculated bond length between the O atom and its bonding Zn atom in the surface is 0.2523 nm, and the O–O bond length of the O_2 molecule is 0.1244 nm. The adsorption structures of O_2 molecule on the perfect ZnO(10$\bar{1}$0) surface are similar in the two theoretical studies, but the calculated adsorption energy has large difference. In our study, the calculated adsorption energy is −28.57 kJ·mol^{-1}, which is only 1.93 kJ·mol^{-1} in reference [15]. We guess that the hydrogen-passivated bottom sides of the ZnO slabs in reference have influence on the adsorption energy. In another study by Yuan et al. [37], the local spin density approximation (LDA) functional has been used to calculate the adsorption of O_2 on the ZnO(10$\bar{1}$0) surface, and an adsorption energy of 57.90 kJ·mol^{-1} is obtained. However, it is generally known that LDA approximation often overestimates the adsorption energy. We also consider other various adsorption structures. O_2(b) is two O atoms of O_2 molecule bridging Zn1 and O1 in a Zn–O bond, the bond lengths of Ob–O1 and Oa–Zn1 are 0.3549 and 0.2212 nm, respectively. The Oa–Ob bond is 0.1260 nm, which is shorter than that in O_2(a). The adsorption energy is −44.05 kJ·mol^{-1}. O_2(c) is two O atoms of O_2 molecule bridging Zn1 and O3 in parasites of a hexagonal channel; the formed Ob–O3 and Oa–Zn1 bonds are 0.2892 and 0.2195 nm, respectively. The Oa–Ob bond is 0.1262 nm, and the adsorption energy is −43.03 kJ·mol^{-1}. Comparing with the O–O bond lengths of adsorbed O_2 molecules and the adsorption energies in three structures, we can see that O_2(a) is the most stable configuration of O_2 adsorption on the perfect ZnO(10$\bar{1}$0) surface, which is fully molecular adsorption.

3.3. Adsorption of SO_2 molecule on the perfect ZnO(10$\bar{1}$0) surface

In the appearance of O_2, S in the sulfurized ZnO(10$\bar{1}$0) surface may react with O_2 leading to the main product SO_2, thus the sulfurized ZnO(10$\bar{1}$0) surface is regenerated. So it is necessary to study the adsorption of SO_2 on the perfect ZnO(10$\bar{1}$0) surface. Six different adsorption configurations of SO_2 on the perfect ZnO(10$\bar{1}$0) surface are obtained, as shown in Fig. 3, and the adsorption energies are listed in Table 1. SO_2(a) is the SO_2 on the top of the surface vertically, the two O atoms bridging two adjacent Zn atoms with an adsorption
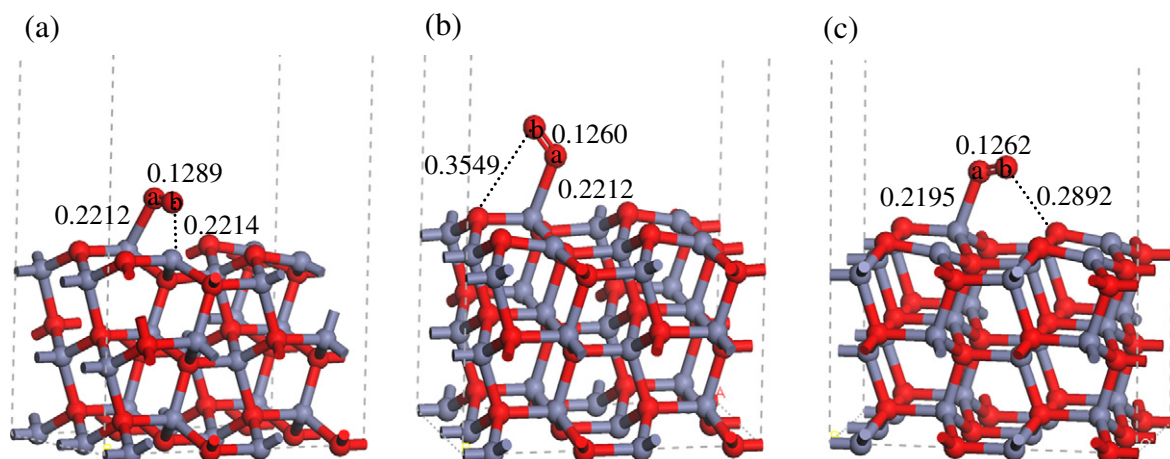

Fig. 2. The adsorption configurations of O_2 molecule on the perfect ZnO(10$\bar{1}$0) surface.

Structures	E_{ads} (kJ·mol^{-1})	Structures	E_{ads} (kJ·mol^{-1})
O_2(a)	−28.57	SO_2(a)	46.94
O_2(b)	−44.05	SO_2(b)	9.66
O_2(c)	−43.03	SO_2(c)	6.81
		SO_2(d)	95.96
		SO_2(e)	95.14
		SO_2(f)	84.60

energy of 46.94 kJ·mol^{-1}, and the O–Zn bonds are 0.2294 and 0.2259 nm, respectively. The adsorption energies of SO_2 in structures SO_2(b) and SO_2(c) are only 9.66 and 6.81 kJ·mol^{-1}, respectively. They are physical adsorption. In SO_2(d), SO_2 lies on the $ZnO(10\bar{1}0)$ surface horizontally, the formed Oa–Zn1 and S–O3 bonds are 0.2061 nm and 0.1988 nm, and the adsorption energy is 95.96 kJ·mol^{-1}. SO_2(e) is S and Oa in SO_2 bonding to O1 and Zn1 on the $ZnO(10\bar{1}0)$ surface, and SO_2 lies on the $ZnO(10\bar{1}0)$ surface horizontally. The adsorption energy is 95.14 kJ·mol^{-1}. In SO_2(f), the S atom bonds to O1, two O atoms of SO_2 bond to two adjacent Zn atoms, and the adsorption energy is 84.60 kJ·mol^{-1}, which is less stable than SO_2(d) and SO_2(e) by 11.36 and 10.54 kJ·mol^{-1}, respectively. It can be seen that SO_2(d) and SO_2(e) are the most stable structures in all adsorption structures of SO_2 on the $ZnO(10\bar{1}0)$ surface, and the second is SO_2(f). In the three structures of SO_2(d), SO_2(e) and SO_2(f), S in SO_2 bonds to a surface oxygen atom to form an analogical SO_3 structure, which is compatible with the report by Chaturvedi et al. [38]. They have studied the reaction

of SO_2 with ZnO surface using synchrotron-based high-resolution photoemission spectroscopy. It shows that the SO_2 molecule probably attaches itself to a surface oxygen atom to form SO_3, and a subsequent reconstruction of the oxide surface produces SO_4. They also investigated the interaction of SO_2 with ZnO(0001)–Zn and ZnO(000$\bar{1}$)–O using ab initio SCF calculations. The theoretical calculations suggest that SO_2 adsorbs on an oxygen site to form SO_3. Prades et al. [39] have also studied the adsorption of SO_2 on the $ZnO(10\bar{1}0)$ surface using the DFT method. The calculated adsorption energy is 108.07 kJ·mol^{-1}, which is similar to our calculation results, but the most stable configuration is two O atoms in SO_2 bonding to a surface Zn atom.

3.4. The regeneration process of the sulfurized $ZnO(10\bar{1}0)$ surface

To obtain further detailed understanding about the regeneration process of the sulfurized $ZnO(10\bar{1}0)$ surface in an oxygen atmosphere, the intermediates and transition states during this process are shown in Figs. 3 and 4. The potential energy profiles for the regeneration process at the GGA–PW91 functional level are shown in Fig. 5 denoted by the black line. As the optimized O_2(a) is the most stable configuration for O_2 adsorption on the perfect $ZnO(10\bar{1}0)$ surface, the coadsorption structure of S and O_2 is configured according to the optimized O_2(a), and the optimized coadsorption structure is shown as IM1 in Fig. 4. In IM1, the S–Zn bond cleavages and S–Oa bond forms, and the bond lengths of Oa–Zn1 and Ob–Zn2 are shorter than that in O_2(a). The formation of IM1 is an exothermic process. Then, IM1 leads to the formation of SO_2(f) via transition state TS1 with an activation energy of 36.79 kJ·mol^{-1}. In this process,
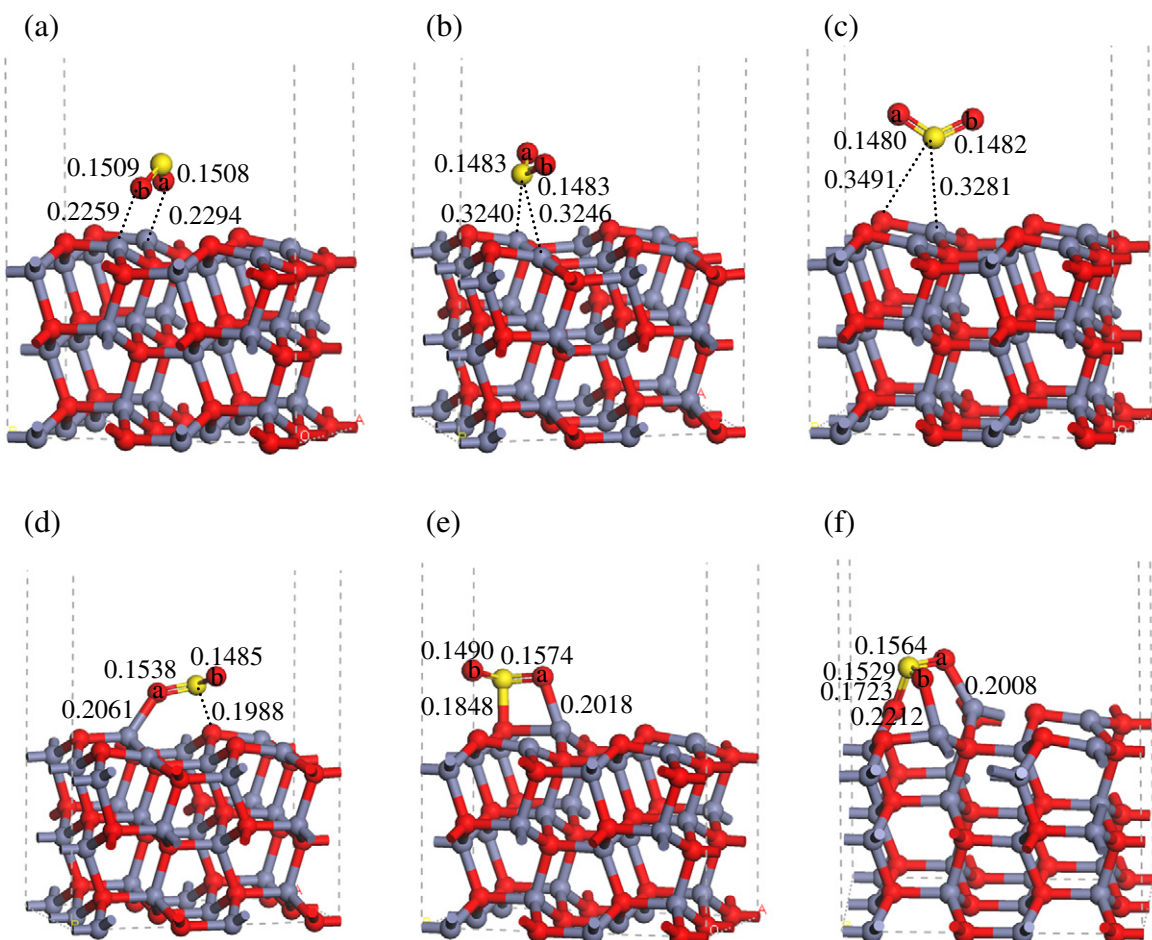

Fig. 3. The adsorption configurations of SO_2 molecule on the perfect $ZnO(10\bar{1}0)$ surface.

the bond length of Ob–Zn2 shortens from 0.1984 nm in IM1 to 0.1853 nm in TS1, then elongates to 0.2212 nm in SO$_2$(f), and the distance between Ob and S shortens to 0.1529 nm in SO$_2$(f). SO$_2$(f) is less stable than SO$_2$(e) by 10.54 kJ·mol^{-1}. The bond of Ob–Zn2 cleavage results in the formation of SO$_2$(e) via TS2 with a little activation energy of 12.22 kJ·mol^{-1}. In this step, the bond length of Ob–S shortens from 0.1529 nm in SO$_2$(f) via 0.1507 nm in TS2 to 0.1490 nm in SO$_2$(e). Comparing with the two steps, we can see that the first step [IM1→SO$_2$(f)] is the rate determining step, and the activation energy is only 36.79 kJ·mol^{-1}. So it can be concluded that the sulfurized ZnO(10$\bar{1}$0) surface is easy to be regenerated in the appearance of O$_2$.

To investigate the influence of different functional levels on the results, the potential energies for the regeneration of the sulfurized ZnO(10$\bar{1}$0) surface have also been calculated using the GGA–BLYP (GGA with the Becke–Lee–Yang–Parr) and LDA–PWC (LDA with the Perdew–Wang correlational) functionals. A comparison of the potential energies at the three functional levels is shown in Fig. 5, and the main bond lengths of intermediates and transition states are listed in Table 2.

We can see that the three functionals have little influence on the bond lengths of all structures. The different functionals yield nearly similar results for the relative reaction energy. The rate determining step for all functionals is IM1→SO$_2$(f), and the activation energies at the GGA–PW91, GGA–BLYP and LDA–PWC levels are 36.79, 29.40 and 44.04 kJ·mol^{-1}, respectively.

3.5. Adsorption of O atom on the perfect ZnO(10$\bar{1}$0) surface

When O$_2$ adsorbs on the oxygen-deficient ZnO(10$\bar{1}$0) surface, one of O atoms can fill the oxygen vacancy in the ZnO(10$\bar{1}$0) surface to make the surface regenerate, and the other O atom adsorbs on the surface. The adsorption mode of O atom on the regenerated ZnO(10$\bar{1}$0) surface, namely the perfect ZnO(10$\bar{1}$0) surface, is needed to understand. The optimized adsorption structures of O atom on the perfect ZnO(10$\bar{1}$0) surface are shown in Fig. 6, the adsorbed O atom is labeled by O*, and the adsorption energies are listed in Table 3. O*(a) is the O* atom bonded to two adjacent Zn atoms of the surface via the bridge bond mode, and two O*–Zn bonds are 0.1950 and 0.1951 nm, respectively. The adsorption energy is 165.26 kJ·mol^{-1}. O*(b) is the O* atom bridging Zn3 and O3 in a Zn–O bond with an adsorption energy of 205.05 kJ·mol^{-1}, the bond length of O*–Zn3 and O*–O3 are 0.1904 and 0.1503 nm, respectively. O*(c) is the O* atom bridging Zn1 and O3 in parasites of a hexagonal channel, and the adsorption energy is 180.71 kJ·mol^{-1}.

Comparing with the adsorption energies of the O* atom on the perfect ZnO(10$\bar{1}$0) surface, the strengths of atomic O adsorption over the three types of adsorption sites could be assigned in the following order, O*(b)>O*(c)>O*(a). It is clear that the O atom
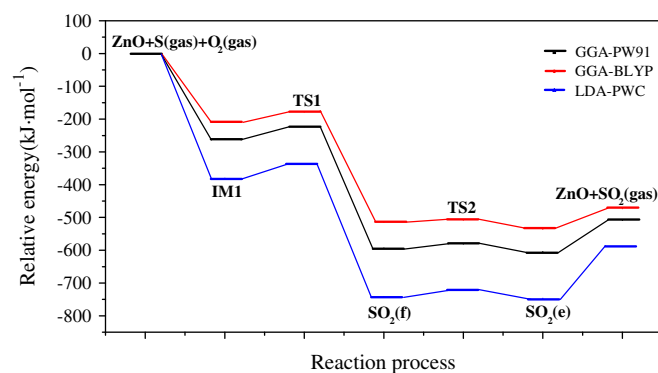

Fig. 5. Potential energy profiles for the regeneration process of the sulfurized ZnO(10$\bar{1}$0) surface. The black line, red line and blue line denote the calculated results at the GGA–PW91, the GGA–BLYP and the LDA–PWC levels, respectively.

bonding to Zn and O in a Zn–O bond is the most stable configuration for single O atom adsorption, which is similar to the adsorption of atomic S on the perfect ZnO(10$\bar{1}$0) surface.

3.6. The regeneration process of the oxygen-deficient ZnO(10$\bar{1}$0) surface

O$_2$ prefers to be adsorbed on the perfect ZnO(10$\bar{1}$0) surface with two O atoms bridging two adjacent Zn atoms. According to this information, the adsorption structures of O$_2$ on the oxygen-deficient ZnO(10$\bar{1}$0) surface are built, shown as M01 and M02 in Fig. 7. In M01, the distances of Ob–Zn3 and Oa–Zn4 are placed as 0.2432 nm and 0.2431 nm, and the distance between two O atoms in O$_2$ molecule is fixed in its free bond length in gas phase (0.1225 nm). Optimized M01 leads to the structure that one atomic oxygen completely fills the original O vacancy on the ZnO(10$\bar{1}$0) surface and the other bridges a Zn–O bond, as shown in M1 in Fig. 7. The bond lengths of Oa–Zn3 and Oa–Ob are 0.1904 and 0.1503 nm, respectively. We find that M1 is the same as O*(b) in Fig. 6, Oa in M1 is corresponding to O* in O*(b), and Ob in M1 is corresponding to O3 in O*(b). When the distances between the O$_2$ molecule and the oxygen-deficient ZnO(10$\bar{1}$0) surface (it is defined as the bond lengths of Ob–Zn3 and Oa–Zn4) are elongated to about 0.3000 nm, the same optimized structure is obtained, which shows that the oxygen-deficient ZnO(10$\bar{1}$0) surface is easy to be regenerated when O$_2$ is on the top of Zn3 and Zn4. The same process was studied by Yan et al. [15], but a bridging O$_2$ adsorption structure is obtained. Our optimized structure does not agree with the report of Yan et al., but we both agree that the oxygen vacancy can promote the dissociation of O$_2$.
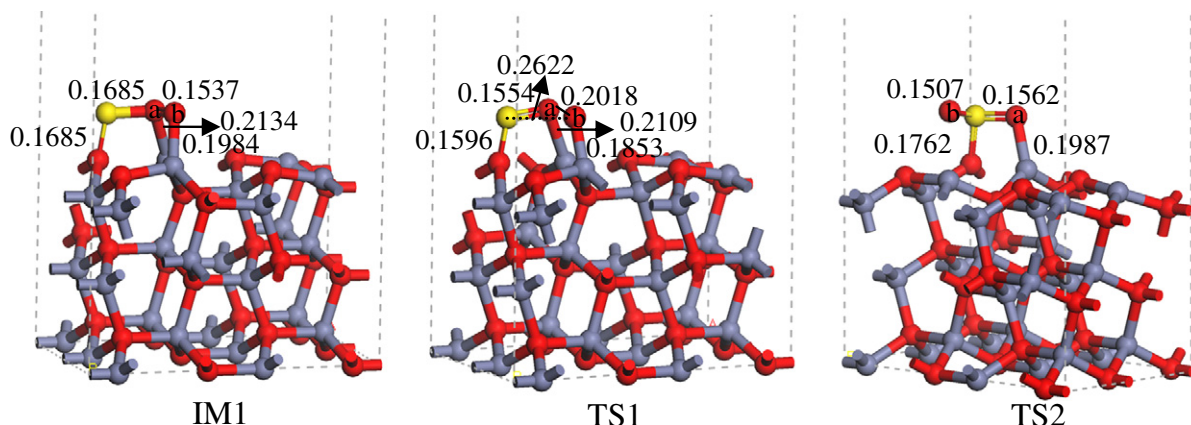

Fig. 4. The intermediates and transition states during the regeneration process of the sulfurized ZnO(10$\bar{1}$0) surface.

Table 2
The main bond lengths of intermediates and transition states during the regeneration of the sulfurized ZnO(10$\bar{1}$0) surface.

Structure	Bond	Bond length (nm)		
		GGA–PW91	GGA–BLYP	LDA–PWC
IM1	S–O_a	0.1685	0.1699	0.1670
	O_a–O_b	0.1537	0.1582	0.1475
	S–O_{surf}	0.1685	0.1699	0.1668
	O_a–Zn_{surf}	0.2134	0.2150	0.2067
	O_b–Zn_{surf}	0.1984	0.1997	0.1944
TS1	S–O_a	0.1554	0.1586	0.1547
	S–O_b	0.2622	0.2651	0.2495
	O_a–O_b	0.2018	0.2081	0.1914
	S–O_{surf}	0.1596	0.1630	0.1596
	O_a–Zn_{surf}	0.2109	0.2107	0.2039
	O_b–Zn_{surf}	0.1853	0.1875	0.1844
SO₂(f)	S–O_a	0.1564	0.1581	0.1544
	S–O_b	0.1529	0.1535	0.1511
	S–O_{surf}	0.1723	0.1752	0.1698
	O_a–Zn_{surf}	0.2008	0.2015	0.1952
	O_b–Zn_{surf}	0.2212	0.2290	0.2164
TS2	S–O_a	0.1562	0.1576	0.1569
	S–O_b	0.1507	0.1518	0.1468
	S–O_{surf}	0.1762	0.1791	0.1730
	O_a–Zn_{surf}	0.1987	0.2004	0.1921
SO₂(e)	S–O_a	0.1574	0.1584	0.1554
	S–O_b	0.1490	0.1495	0.1489
	S–O_{surf}	0.1848	0.1926	0.1754
	O_a–Zn_{surf}	0.2018	0.2043	0.1987

Table 3
The adsorption energies of O atom on the perfect ZnO(10$\bar{1}$0) surface.

Structures	E_{ads} (kJ·mol⁻¹)
O*(a)	165.26
O*(b)	205.05
O*(c)	180.71

The other structure of O_2 molecule placed on the top of two adjacent Zn atoms is built, as shown in M02 in Fig. 7. The distances between Ob and Zn5, Oa and Zn6 are placed as 0.2437 nm and 0.2430 nm, which are larger than that of the bonding distance between Zn and O (about 0.2240 nm). M2 is the optimized structure of M02; we can see that the Oa and Ob both insert into the O vacancy site, and Ob bonds to Zn1, Zn5 and Oa, as well as Oa bonds to Zn3, Zn6 and Ob. In M2, the bond lengths of Ob–Zn1, Ob–Zn5, Oa–Zn3 and Oa–Zn6 are 0.2165, 0.2006, 0.1940, and 0.2027 nm, respectively. The distance between Oa and Ob is 0.1499 nm, which is longer than that of O_2 in gas phase by 0.0274 nm. It shows that the O_2 molecule is elongated and the oxygen-deficient surface promotes the dissociation of O_2. The ZnO(10$\bar{1}$0) surface has not been regenerated via M02 optimizing. Then, we investigate the process of M2 conversing to O*(b) because it is the most stable configuration of O* adsorption on the perfect ZnO(10$\bar{1}$0) surface. A little activation energy of 29.43 kJ·mol⁻¹ is needed in this step via transition state TS3. In this step, the bond length of Oa–Zn3 changes from 0.1940 nm in M2 to 0.1904 nm in O*(b) via 0.1899 nm in TS3 (Oa is corresponding to O*), and the Ob–Oa changes from 0.1499 nm in M2 to 0.1503 nm

in O*(b) via 0.1470 nm in TS3 (Ob is corresponding to O3). So we can see that the oxygen-deficient ZnO(10$\bar{1}$0) surface is easy to be regenerated when O_2 is on the top of Zn5 and Zn6.

The above two regeneration processes show that the oxygen-deficient ZnO(10$\bar{1}$0) surface is easy to be regenerated in an oxygen atmosphere. Comparing with the adsorption of O_2 on the perfect and oxygen-deficient ZnO(10$\bar{1}$0) surface, it can be seen that the oxygen vacancy on the surface dominates the chemical properties and the adsorption behaviors of ZnO, which is compatible with the previous result [15].

4. Conclusions

Density functional theory calculations have been carried out to investigate the regeneration mechanisms of the sulfurized and oxygen-deficient ZnO(10$\bar{1}$0) surfaces during the desulfurization of H_2S by ZnO. For the sulfurized ZnO(10$\bar{1}$0) surface, there are two steps in the regeneration process. The activation energy of the rate determining step is only 36.79 kJ·mol⁻¹ at the GGA–PW91 functional level, which shows that the sulfurized ZnO(10$\bar{1}$0) surface can be regenerated easily. The formed SO_2 lies on the ZnO(10$\bar{1}$0) surface horizontally; the S atom of SO_2 bonds to a surface oxygen atom to from an analogical SO_3 structure, which is compatible with the report by Chaturvedi et al. [38].

Two regeneration mechanisms are considered for the oxygen-deficient ZnO(10$\bar{1}$0) surface. One mechanism is that O_2 dissociatively adsorbs on the oxygen-deficient ZnO(10$\bar{1}$0) surface, where one O atom of O_2 fills the oxygen vacancy site, and the other bridges Zn and O in a Zn–O bond, which is the most stable configuration of the O atom adsorbing on the perfect ZnO(10$\bar{1}$0) surface. The other mechanism is that O_2 molecularly adsorbs on the oxygen-deficient ZnO(10$\bar{1}$0) surface, and the bond length of O–O is elongated. Then, an activation energy of 29.43 kJ·mol⁻¹ is needed to make the surface regenerate. Our results show that the oxygen-deficient ZnO(10$\bar{1}$0) surface is easy to be regenerated in an atmosphere containing O_2.
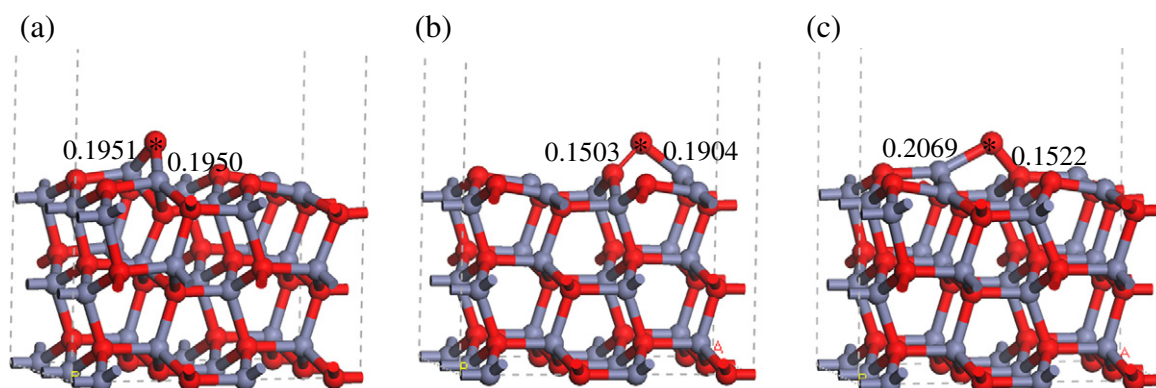
Fig. 6. The adsorption configurations of O* atom on the perfect ZnO(10$\bar{1}$0) surface.
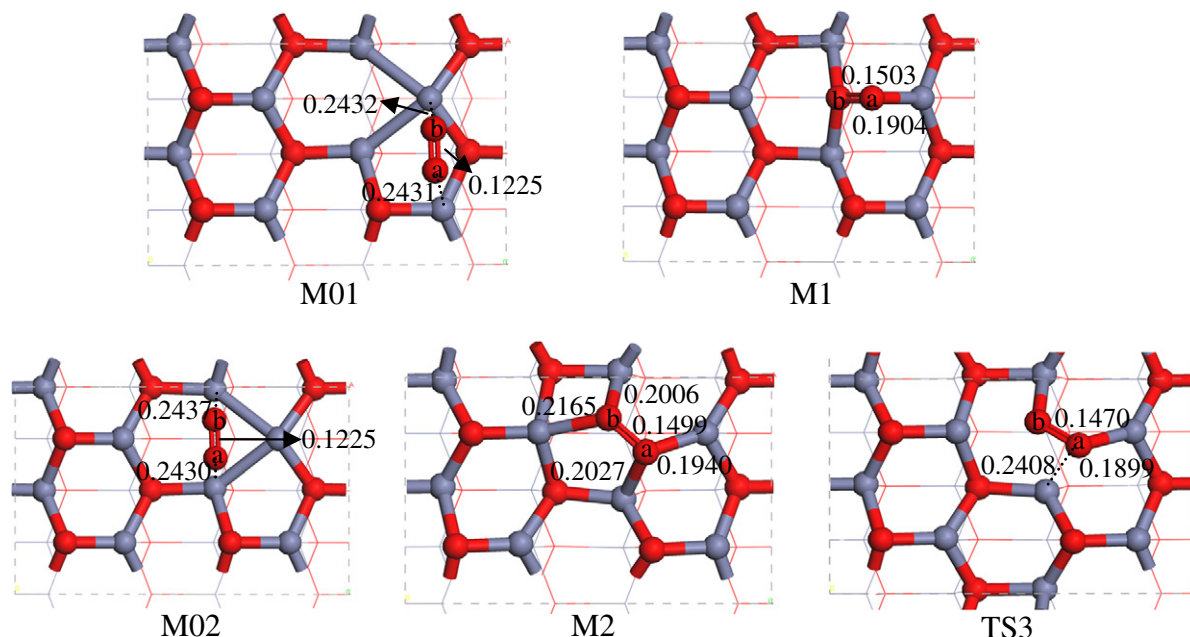
Fig. 7. The original adsorption structures (M01 and M02), optimized structures (M1 and M2) and transition states (TS3) of O_2 on the oxygen-deficient ZnO(10$\bar{1}$0) surface.

References

[1] I.I. Novochinskii, C.S. Song, X.L. Ma, X.S. Liu, L. Shore, J. Lampert, R.J. Farrauto, Low-temperature H₂S removal from steam-containing gas mixtures with ZnO for fuel cell application. 1. ZnO particles and extrudates, Energy & Fuels 18 (2004) 576–583.
[2] H.Y. Yang, R. Sothen, D.R. Cahela, B.J. Tatarchuk, Breakthrough characteristics of reformate desulfurization using ZnO sorbents for logistic fuel cell power systems, Industrial and Engineering Chemistry Research 47 (2008) 10064–10070.
[3] W.F. Elseviers, H. Verelst, Transition metal oxides for hot gas desulphurization, Fuel 78 (1999) 601–612.
[4] S.S. Tamhankar, M. Bagajewlcz, G.R. Gavalas, P.K. Sharma, M. Flytzanl-Stephanopoulos, Mixed-oxide sorbents for high-temperature removal of hydrogen sulfide, Industrial and Engineering Chemistry Process Design and Development 25 (1986) 429–437.
[5] S. Lew, K. Jothimurugesan, M. Flytzani-Stephanopoulos, High-temperature H₂S removal from fuel gases by regenerabel zinc oxide-titanium dioxide sorbents, Industrial and Engineering Chemistry Research 28 (1989) 535–541.
[6] D.R. Kidd, G.A. Delzer, D.H. Kubicek, P.F. Schubert, Selective removal of hydrogen sulfide over a zinc oxide and silica absorbing composition, US patent no. 5358921 (1994).
[7] G.D. Focht, P.V. Ranade, D.P. Harrison, High-temperature desulfurization using zinc ferrite: regeneration kinetics and multicycle testing, Chemical Engineering Science 44 (1989) 2919–2926.
[8] S. Cheah, D.L. Carpenter, K.A. Magrini-Bair, Review of mid- to high-temperature sulfur sorbents for desulfurzation of biomass- and coal-derived syngas, Energy & Fuels 23 (2009) 5291–5307.
[9] P.C. Colombes, A.D. Noisy-le-Roi, S. Franckowiak, A. Sugier, R. Malmaison, Process for purifying a gas containing hydrogen sulfide and contact masses usable therefor. US patent no. 4088736 (1978).
[10] L.N. Kantorovich, M.J. Gillan, Adsorption of atomic and molecular oxygen on the MgO(001) surface, Surface Science 374 (1997) 373–386.
[11] Y.J. Xu, J.Q. Li, Y.F. Zhang, W.K. Chen, Theoretical study of O₂ adsorption on perfect and defect sites of MgO(001) surface, Acta Physico-Chimica Sinica 19 (2003) 414–418.
[12] F.R. Sensato, R. Custódio, M. Calatayud, A. Beltrán, J. Andrés, J.R. Sambrano, E. Longo, Periodic study on the structural and electronic properties of bulk, oxidized and reduced SnO₂(110) surfaces and the interaction with O₂, Surface Science 511 (2002) 408–420.
[13] D. Le, S. Stolbov, T.S. Rahman, Reactivity of the Cu₂O(100) surface: insights from first principles calculations, Surface Science 603 (2009) 1637–1645.
[14] R.G. Zhang, H.Y. Liu, H.Y. Zheng, L.X. Ling, Z. Li, B.J. Wang, Adsorption and dissociation of O₂ on the Cu₂O (111) surface: thermochemistry, reaction barrier, Applied Surface Science 257 (2011) 4787–4794.
[15] Y.F. Yan, M.M. Al-Jassim, S.H. Wei, Oxygen-vacancy mediated adsorption and reactions of molecular oxygen on the ZnO(10Ī0) surface, Physical Review B 72 (2005) (161307-1-4).
[16] M. Kroll, T. Kuschel, T. Löber, U. Köhler, Large scale morphology of ZnO(10Ī0) surface, Surface Science 603 (2009) L49–L51.
[17] N. Jedrecy, S. Gallini, M. Sauvage-Simkin, R. Pinchaux, The ZnO non-polar (10Ī0) surface: an X-ray structural investigation, Surface Science 460 (2000) 136–143.
[18] N.L. Marana, V.M. Longo, E. Longo, J.B.L. Martins, J.R. Sambrano, Electronic and structural properties of the (100) and (110) ZnO surface, Journal of Physical Chemistry A 112 (2008) 8958–8963.
[19] J. Hu, W.P. Guo, X.R. Shi, B.R. Li, J.G. Wang, Copper deposition and growth over ZnO nonpolar (100) and (110) surfaces: a density functional theory study, Journal of Physical Chemistry C 113 (2009) 7227–7235.
[20] L.X. Ling, R.G. Zhang, P.D. Han, B.J. Wang, DFT study on the sulfurization mechanism during the desulfurization of H₂S on the ZnO desulfurizer, Fuel Processing Technology (2012) (http://dx.doi.org/10.1016/j.fuproc.2012.08.001).
[21] Y.F. Yan, M.M. Al-Jassim, Structure and energetics of water adsorbed on the ZnO(10Ī0) surface, Physical Review B 72 (2005) (235406-1-6).
[22] P. Ordejón, E. Artacho, J.M. Soler, Selfconsistent order-N density-functional calculations for large systems, Physical Review B 53 (1996) R10441–R10444.
[23] D. Sánchez-Portal, P. Ordejón, E. Artacho, J.M. Soler, Density-functional method for very large systems with LCAO basis sets, International Journal of Quantum Chemistry 65 (1997) 453.
[24] J.P. Perdew, K. Burke, M. Ernzerhof, Generalized gradient approximation made simple, Physical Review Letters 77 (1996) 3865–3868.
[25] J.P. Perdew, K. Burke, Y. Wang, Generalized gradient approximation for the exchange-correlation hole of a many-electron system, Physical Review B 54 (1996) 16533–16539.
[26] P. Hohenberg, W. Kohn, Inhomogeneous electron gas, Physical Review B 136 (1964) B864–B871.
[27] M. Dolg, U. Wedig, H. Stoll, H. Preuss, Energy-adjusted ab initio pseudopotentials for the first row transition elements, Journal of Chemical Physics 86 (1987) 866–872.
[28] B. Delley, Form molecules to solids with the Dmol³ approach, Journal of Chemical Physics 113 (2000) 7756–7764.
[29] B. Delley, An all-electron numerical method for solving the local density functional for polyatomic molecules, Journal of Chemical Physics 92 (1990) 508–517.
[30] T.A. Halgren, W.N. Lipscomb, The synchronous-transit method for determining reaction pathways and locating molecular transition states, Chemical Physics Letters 49 (1977) 225–232.
[31] D.R. Lide, in: Handbook of Chemistry and Physics, 82nd, CRC Press, Boca Raton, 2001–2002, pp. 9–23.
[32] R.G. Zhang, H.Y. Liu, B.J. Wang, J. Ren, Z. Li, Adsorption and dissociation of O₂ on CuCl(111) surface: a density functional theory study, Applied Surface Science 258 (2011) 408–413.
[33] H. Sawada, R. Wang, A.W. Sleight, An electron density residual study of zinc oxide, Journal of Solid State Chemistry 122 (1996) 148–150.

[34] M.J.S. Spencer, K.W.J. Wong, I. Yarovsky, Density functional theory modeling of ZnO(10$\bar{1}$0) and ZnO(11$\bar{2}$0) surfaces: structure, properties and adsorption of N2O, Materials Chemistry and Physics 119 (2010) 505–514.

[35] B. Meyer, D. Marx, Density-functional study of the structure and stability of ZnO surfaces, Physical Review B 67 (2003) (035403-1-11).

[36] C.B. Duke, R.J. Meyer, A. Paton, P. Mark, Calculation of low-energy-electron-diffraction intensities from ZnO(10$\bar{1}$0). II. Influence of calculational procedure, model potential, and second-layer structural distortions, Physical Review B 18 (1978) 4225–4240.

[37] Q.Z. Yuan, Y.P. Zhao, L.M. Li, T.H. Wang, Ab initio study of ZnO-based gas-sensing mechanisms: surface reconstruction and charge transfer, Journal of Physical Chemistry C 113 (2009) 6107–6113.

[38] S. Chaturvedi, J.A. Rodriguez, T. Jirsak, J. Hrbek, Surface chemistry of SO_2 on Zn and ZnO: photoemission and molecular orbital studies, The Journal of Physical Chemistry. B 102 (1998) 7033–7043.

[39] J.D. Prades, A. Cirera, J.R. Morante, Ab initio calculation of NO_2 and SO_2 chemisorption onto non-polar ZnO surfaces, Sensors and Actuators B 142 (2009) 179–184.